1024 3D-stacked monolithic NEMS array with 375μm 2 0.5mw 0.28ppm frequency deviation pixel-level readout for zeptogram gravimetric sensing

Gérard Billiot, Paul Mattei, Bogdan Vysotskyi, Adrien Reynaud, Louis Hutin, Christophe Plantier, Emmanuel Rolland, Marc Gely, Giulia Usai, Claude Tabone, et al.

12.7 1024 3D-Stacked Monolithic NEMS Array with 375µm2 0.5mW 0.28ppm Frequency Deviation Pixel-level Readout for Zeptogram Gravimetric Sensing

Gérard Billiot, Paul Mattei, Bogdan Vysotskyi, Adrien Reynaud, Louis Hutin, Christophe Plantier, Emmanuel Rolland, Marc Gely, Giulia Usai, Claude Tabone, Gaël Pillonnet, Stéphanie Robinet, Sébastien Hentz

CEA-Léti, Grenoble, France

NanoElectroMechanical System (NEMS)-based resonator sensors are a promising approach to detect a single molecule deposition with zeptogram mass resolution [1]. However, MEMS sensing areas (1's µm²) are several orders of magnitude lower than the mass deposition focus beam (mm²-scale), dramatically reducing the probability of detecting molecules, thus increasing the detection time [2]. NEMS and CMOS co-integration has already been considered but the density NEMS arrays limits the detection probability and scalable readout circuits fully suitable to NEMS pixel constraints e.g. size, power consumption, resolution has not been proposed yet. We propose the first realization of a fully 3D-monolithic 1024 zepto-balances (zBal) array including NEMS-based gravimetric sensor [2] and readout circuits individually addressed by on-chip matrix decoder and voltage drivers and controlled by a shared phase-locked loop which scans sequentially two resonant frequencies of each NEMS. We report a zBal readout with 0.5 mW power-consumption, 375 µm², silicon footprint and 0.28 ppm frequency-resolution variability for a 10 ms individual NEMS acquisition time. The 0.7 % frequency variability measured on 1024 NEMS arrays allows higher effective sensing area than the previously published active NEMS sensors [3]–[5].

Existing readout schemes rely on tracking phase [2,4,6] or frequency shift [3] by using a phase-locked loop (PLL) and a self-oscillating loop (SOL), respectively. Even if the SOL scheme seems to be the most compact option to address a NEMS array in parallel, as only an amplifier and a phase-shifter are required, previous works show the prohibitive Si footprint of a single [3,6] or heterodyne [4] SOL compared to the NEMS area (2.5 µm²) which tends to decrease with the 3D interconnect density improvement. Here, we use the restrictive Si area above NEMS resonator only to integrate monolithically a low noise amplifier (LNA) and matrix decoder and we mutualize the PLL feedback to sequentially address each zBal. A mutualized SOL scheme cannot be chosen as the array's trace impedance from the interconnection network would affect the resonant frequency tracking accuracy [3].

The 3D-stacked monolithic integration of 1024 NEMS above the readout to address the NEMS array is illustrated in Fig. 1. 8192 NEMS-to-IC interconnections are performed by 1 µm diameter vias. 1024 doubly pinned beam NEMS (10x0.3x0.16 µm) [2] and 8 pads (10x25 µm total area) have been fabricated above a 5V-130nm CMOS process integrating zBal readout composed of a LNA to adapt the NEMS output impedance and increase the NEMS output voltage (U_S~100 µV). Only 6 signals are exchanged with a shared lock-in amplifier (LIA) which sequentially scans each $zBal_{i,j}$ thanks to the on-chip matrix decoder including LNA load, row/column decoders and voltage drivers (U_{Am}~100's mV). Figure 1 and 7 also depict top and side views of the 3D stacked NEMS-CMOS chip.

Fig. 2 shows the pixel- and row-level phase-based readout scheme with a shared and external PLL feedback (LIA lab-instrument). The NEMS are sequentially actuated at their two first mechanical resonant frequencies $\{F_{A1},F_{A2}\}$ located around 28 MHz and 75 MHz, by U_{A1} and U_{A2} actuation pads. Four nanowire gauges biased by U_G@F_G down-mix the U_A signals. The sensing signal U_S rated at F_A-F_G (F_S~100 kHz to avoid 1/F noise [2]) generated by the mixing effect of the 2 kΩ piezoresistive bridge is amplified at pixel-level by a LNA and sent to the LIA's input ADC (12 bits ENOB, 500 MSPS) through the on-chip matrix decoder. Then IQ modulation is performed to extract the U_S phase $\varphi_{i,j}$ of the $zBal_{i,j}$ and compare it to a referenced phase $\varphi_{i,j,REF}$ corresponding to resonance prior to mass deposition. $\Delta\varphi$ is maintained to zero thanks to the PLL controller (tunable PID) which the convergence time is set by its time constant θ. Two frequency generation blocks (1 mHz frequency resolution DDS) and DAC (14 bits ENOB, 1 GSPS) deliver the actuation U_{Am} and gauge signals U_G to track the resonant frequency with zero-phase lock. Actuator DDS is initialized by the pre-characterized resonant frequency $\{F_{A,REF}\}_{i,j}$ to ensure a locked PLL operation and fast convergence. More details in the sensing principle are given in [2]. A selectable LNA composed of a differential NMOS pair (DP) is integrated below each NEMS. The LNA active loads (AL) are mutualized per row to reduce the footprint. The amplifier stage formed by DP and AL has 15 dB voltage-gain and 2 MHz unity-gain-bandwidth (GBW) product and consumes 0.5 mW under 3 V power supply. The DP size is 38/0.5 µm to achieve 30 nV/√Hz noise level @100 kHz, sufficient GBW (GBW>>F_S) and low input capacitance.

An initial array mapping is performed to acquire the two resonant frequencies and phases without mass deposition as shown in Fig. 3 for $zBal_{9,10}$ by scanning the zBal array in a PLL open-loop configuration. Due to the process variability, the resonance frequencies, quality factor and LNA voltage gain of each zBal vary as shown in Fig. 4. The F_{Am} variability is limited to 0.7 % @1σ showing the fairly good process reproducibility. The reference frequency and phase of the two resonant modes of 1024 zBal are screened and serve to set initial conditions during zBal matrix scan. The frequency shift between the measured frequency in closed-loop $\{F_{Am}\}_{i,j}$ and $\{F_{Am,REF}\}_{i,j}$ is linked to a mass deposition on the $NEMS_{i,j}$. The combination of the two resonant frequency shifts (F_{A1}, F_{A2}) allows to determine the mass and its position on the doubly-pinned beam NEMS as described in [2].

Closed-loop measurements into a vacuum chamber are reported in Fig. 5. The scanning sequence composed by the first and second resonant frequencies of four zBal shows the locked operation of PLL as a low phase shift $\Delta\varphi$ is maintained. The F_{A2} frequency shift is also shown for two emulated mass deposition events. Again, the locked-phase operation of PLL is maintained. The minimal settling time to sense the frequency shift is 4 ms due to the time constant of the PLL control. The frequency variation characterized by the Allan deviation is a major criteria to evaluate the achievable mass resolution [2]. Fig. 5 depicts the deviation in open loop operation for several beams – chosen randomly within the same array – and confirms the fabrication reliability. The ultimate 0.15 ppm frequency variation for an integration time of 10 ms would yield a 170 zg mass resolution at room temperature. The array screening can be as fast as 1 ms by setting θ to 500 ns while maintaining sub-attogram mass resolution. The frequency shift due to the emulation of mass deposition using voltage biasing on the gauges is also reported in Fig. 5.

Fig. 6 compares the major previously published results for mass sensing application. We are the first to experimentally characterize a co-integrated readout circuitry compatible with the NEMS pixel area allowing a sequential scan of 1024 NEMS-based mass sensors. The proposed circuit sequentially tracks the two resonance modes with the lowest reported pixel-level readout power consumption for the lowest frequency resolution allowed by our shared-PLL approach. The 1 ms settling time and 0.28 ppm Allan variation allow up to 170 zg mass resolution and MEMS matrix scanning. The matrix structure increases the effective sensing area compared to the single NEMS already published and opens the way to the industrial adoption of NEMS-CMOS co-integration for mass sensing.

Acknowledgements:
This work was partially funded by ERC ENLIGHTENED.

References:

[1] S. Dominguez-Medina et al., "Neutral mass spectrometry of virus capsids above 100 megadaltons with nanomechanical resonators", *Science*, vol. 362, issue 6417, pp. 918-922, Nov. 2018.

[2] E. Sage et al., "Neutral particle mass spectrometry with nanomechanical systems," *Nature Commun.*, vol. 6:6482, pp. 1-5, Nar. 2015.

[3] G. Arndt et al., "Towards ultra-dense arrays of VHF NEMS with FDSOI-CMOS active pixels for sensing applications," *ISSCC Dig. Tech. Papers*, pp. 320-322, Feb. 2012.

[4] N. Delorme et al., "A NEMS-array control IC for sub-attogram gravimetric sensing applications in 28nm CMOS technology," *ISSCC Dig. Tech. Papers*, pp. 298-299, Feb. 2015.

[5] G. Gourlat et al., "A 30-to-80MHz simultaneous dual-mode heterodyne oscillator targeting NEMS array gravimetric sensing applications with a 300zg mass resolution," *ISSCC Dig. Tech. Papers*, pp. 266-267, Feb. 2017.

[6] K. Bholasle et al., "Standard CMOS integrated ultra-compact micromechanical Oscillating active pixel arrays," MEMS, pp. 157-160, Jan. 2021.

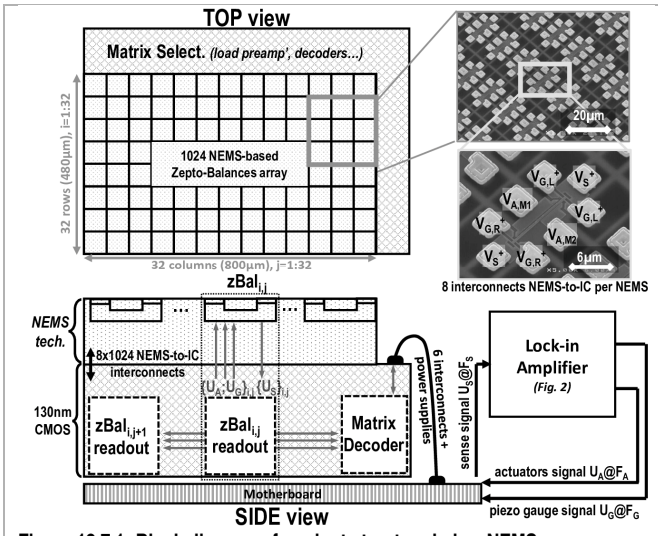

Figure 12.7.1: Block diagram of readout structure below NEMS array.

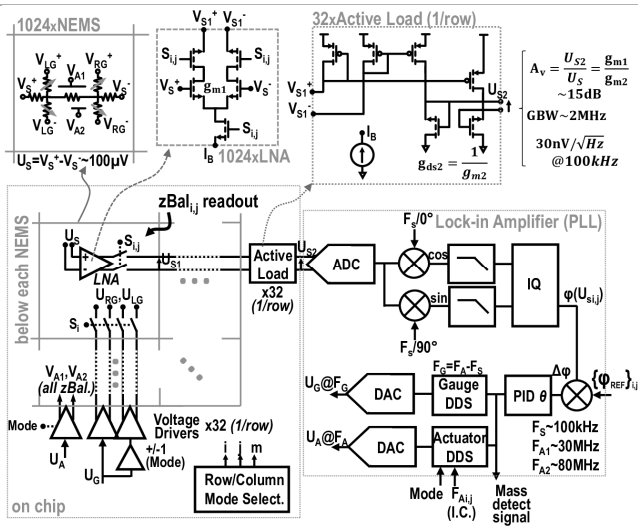

Figure 12.7.2: Simplified circuit schematic in the array and PLL architecture.

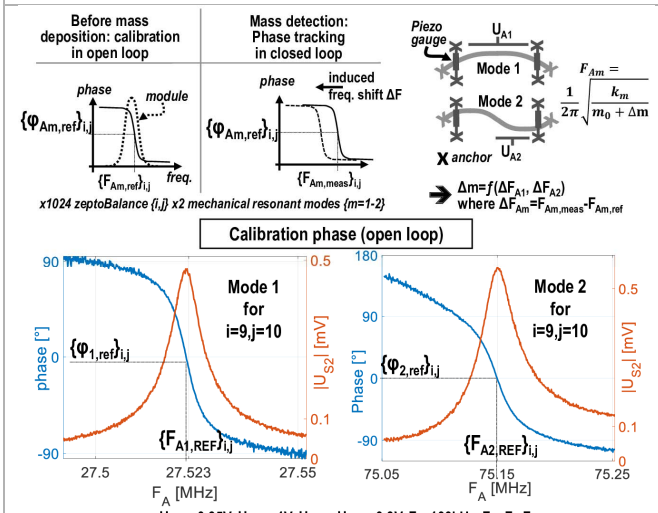

Figure 12.7.3: Readout principle and measured open-loop frequency responses.

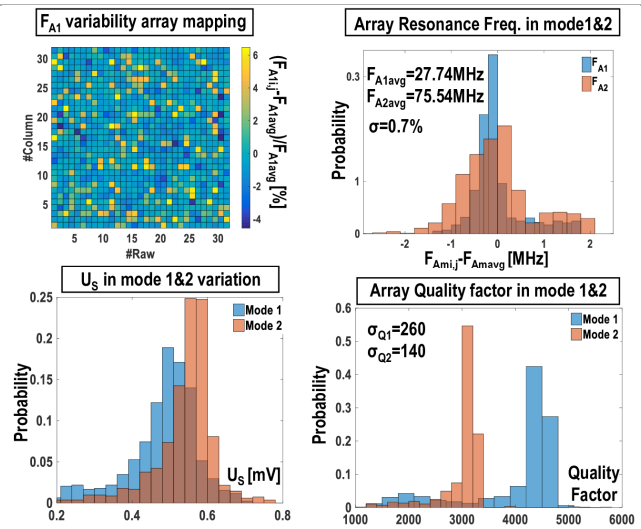

Figure 12.7.4: Measured zepto-balances array mapping performance.

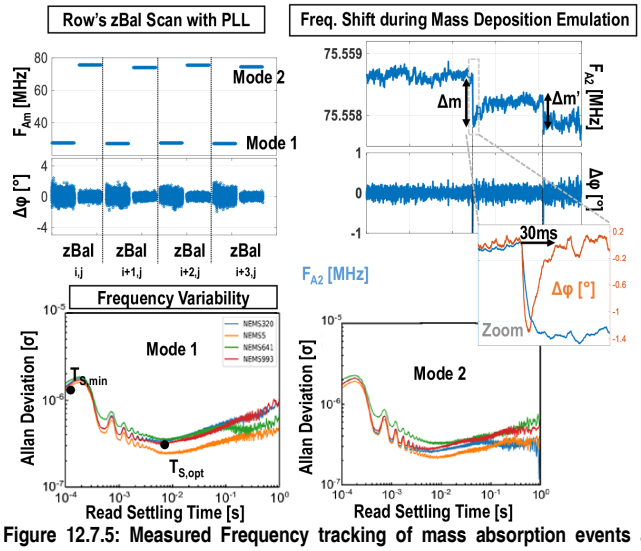

Figure 12.7.5: Measured Frequency tracking of mass absorption events and Allan deviations.

	Nat. Com'15 [2]	ISSCC'12 [3]	ISSCC'15 [4]	ISSCC'17 [5]	MEMS'21 [6]	This Work	Unit
NEMS detection	mass	gas	gas	mass	-	mass	-
# NEMS matrix	1	1	4	1	6	**1024**	-
NEMS & readout packaging	PCB	single die 2D	two dice	two dice	single die	single die **3D**	-
Readout topology	PLL	SOL	PLL	H-SOL	PLL	PLL	-
Closed loop	Yes	No	Yes	Yes	Yes	Yes	-
IC Si technology	stand-alone	300nm	28nm	130nm	350nm BEOL	130nm Monolitic 3D	-
Pixel readout die size	NA	900	1 000 000	26 000	2000	**375***	µm²
Freq. resolution	**80**	NC	800	300	2000	280	x10⁻⁹
Mass resolution	**120**	NA	NA	300	-	170	zg
Min. readout time	10	NC	100	2	-	**1**	ms
Pixel Readout Power consumption	NC	NC	68	3.3	0.09-1.7■	0.5	mW
1024 NEMS + readout area	NA	NA	500**	2**	4,3**	**0.73**	mm²

** Composed by LNA and multiplexer ** Prospective ■ power vs freq resolution cannot be extracted from [6]*

Figure 12.7.6: Summary and comparison to state of the art.

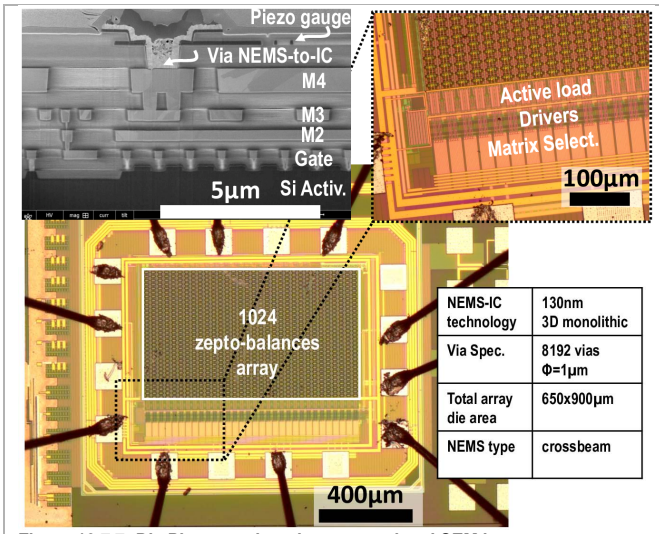

Figure 12.7.7: Die Photograph and cross-sectional SEM image.